

Increase of electrical conductivity with pressure as an indicator of conduction through a solid phase in midcrustal rocks

T. J. Shankland

Earth and Environmental Science Division, Los Alamos National Laboratory, Los Alamos, New Mexico

A. G. Duba

Geosciences and Global Security Program, Lawrence Livermore National Laboratory, Livermore, California

E. A. Mathez and C. L. Peach¹

Department of Earth and Planetary Sciences, American Museum of Natural History, New York

Abstract. Rocks freshly cored from depth at the German continental scientific drilling site (KTB) offer an opportunity to study transport properties in relatively unaltered samples resembling material in situ. Electrical conductivity σ was measured to 250 MPa pressure, and room temperature on 1 M NaCl-saturated amphibolites from 4 to 5 km depth. An unexpected feature was an increase of σ with pressure P that appeared (anisotropically) in most samples. To characterize this behavior, we fitted the linear portion of $\log\sigma$ versus P to obtain two parameters: the slope $d\log\sigma/dP$ (of order 10^{-3} MPa^{-1}) and the zero-pressure intercept σ_0 . Samples of positive and negative slopes behave differently. Those having negative slopes show strong correlation of σ_0 with a fluid property (permeability). This behavior indicates that fluids exert the dominant control on σ_0 at low pressure when σ_0 is greatest, which is typical behavior observed in previous studies. In contrast, samples with positive slopes lack a correlation of σ_0 with permeability, indicating that fluids are less important to positive pressure behavior. Another result is that samples of negative $d\log\sigma/dP$ have uncorrelated slopes and initial conductivities. In significant contrast, samples of positive slopes have the greatest P dependence for lowest initial conductivity σ_0 , that is, the less fluid, the more positive $d\log\sigma/dP$. Hence positive $d\log\sigma/dP$ is consistent with reconnection of solid phases into a conductive texture better resembling that of rock at depth. Detailed examination of one sample by electron probe and scanning electron microscope reveals the presence of carbon on internal cleavage surfaces in amphibole, the most abundant mineral present. Thus carbon probably dominates the reconnection, but total σ still involves fluids as well as Fe-Ti oxides. For the KTB location it is inferred that the reason mid to deep crustal electrical conductivities modeled from geophysical measurements are so much higher than conductivities of silicates is the presence of interconnected good conductors involving films of carbon on surfaces and other solid phases.

Introduction

A persistent problem in interpreting geophysical electrical conductivity σ has been relating it to conductivities measured in the laboratory. The most abundant crustal silicates at crustal temperatures are nearly always more insulating by orders of magnitude than are crustal conductivities from geophysical models [Kariya and Shankland, 1983; Olhoeft, 1981a; Lee et al., 1983; Brace, 1971]. The common remedy has been to invoke the presence of a material of higher electrical conductivity that may not be present in samples measured in the laboratory but that are known to exist in the field. Table 1 suggests orders of magnitude for a few materials that may impart high conductivity together with minimum volume fractions required to obtain conductivities of the order of 10^{-2} S m^{-1} . The presumption for a minimum volume fraction

is nearly linear dependence on volume fraction of the conducting phase as in parallel alignment of conductors or in effective medium theory [Waff, 1974; Madden, 1976].

Different means for enhancing mid and lower crustal conductivities have been argued for some time [e.g., Haak and Hutton, 1986; Schwarz 1990; Jödicke, 1992; Jones, 1992; Frost and Bucher, 1994, Hyndman et al., 1993]. Numerous workers have attributed crustal conductivity to fluid-filled porosity [e.g., Brace, 1971; Frost and Bucher, 1994, Olhoeft, 1981b; Shankland and Ander, 1983; Gough, 1986; Bailey et al., 1989; Hyndman and Shearer, 1989]. Jiracek [1995] and Jiracek et al. [1995] have summarized the case for conduction by fluids at lithostatic pressure beneath a ductile cap zone. Although partial melt is another possibility, it is not expected outside regions of recent volcanic/tectonic activity. Solid phases such as ore minerals or graphite have also been known to produce zones of high conductivity, but they usually have been regarded as special rather than ubiquitous features of the mid to lower crust. Mapping of carbon films by Auger electron emission from metamorphic rocks [Frost et al., 1989; Katsube and Mareschal, 1993] together with the suggestion that connection of the films had been broken by unloading and

¹Now at Sea Education Association, Woods Hole, Massachusetts.

Table 1. Electrical Conductivity of Some Conductive Phases and the Minimum Amount of Each Required to Attain Geophysically Significant Conductivities

Conductor	Conductivity, $S\ m^{-1}$	Minimum Volume Fraction for $0.01\ S\ m^{-1}$
Seawater ($\sim 1\ M\ NaCl$)	~ 3	~ 0.03
Silicate Melt	~ 3	~ 0.03
Sulfides	$\sim 10^2$	$\sim 10^{-4}$
Ilmenite	$\sim 10^3$	$\sim 10^{-5}$
Carbon	$\sim 10^4$	$\sim 10^{-6}$

As most of these quantities can vary extremely depending on geological conditions, they should be taken as guidelines.

alteration as the rock was uplifted to the surface [Duba, 1992; Katsube and Mareschal, 1993] enhanced interest in the potential of carbon to influence crustal conductivity. As can be seen in Table 1, the exceptionally high conductivity of graphite or amorphous carbon means that only small amounts are necessary; further, several geochemical means for widespread deposition of such films had been hypothesized [Mathez and Delaney, 1981; Mathez, 1987; Sanders, 1991; Tingle et al., 1991; Walther and Althaus, 1993; Mareschal et al., 1992; Mathez et al., 1995]. A persistent problem has been that samples have rarely been available from the few documented regions having conductivities attributed to carbon [e.g., Alabi et al., 1975; Sternberg, 1979; Haak et al., 1991; Jödicke, 1992], with the exception of black shales [Duba et al., 1988] from the north German conductivity anomaly [Losecke et al., 1979]. The latter, however, do not speak to the broader issue of conductivities of crystalline rocks. Freshly cored samples from the German continental scientific drilling site (KTB) now provide an opportunity to examine the solid conductor hypothesis [Duba et al., 1994] in more detail. The approach adopted here is to investigate

relationships between conductivity behaviors of the rocks and to demonstrate distributions of the phases that can influence conductivity. In particular, we show that the sign (positive or negative) of the pressure change of conductivity can be used to interpret conduction mechanisms, and the slope is a diagnostic of interconnection of conducting elements.

Experimental Methods

This paper presents new, extended analyses of data from original KTB measurements by Nover et al. [1995]. Electrical conductivity was measured at room temperature as a function of frequency between $\approx 1\ kHz$ and $1\ MHz$ and at hydrostatic pressures to $250\ MPa$ on randomly selected metamorphic rocks cored from depths between 4.1 and $7.0\ km$ in the main Hauptbohrung and one from $1858\ m$ deep in the pilot hole Vorbohrung, both at the KTB site in Windischeschenbach, Germany. The KTB was drilled into the western margin of the Bohemian Massif in northeastern Bavaria, central Germany [Emmermann et al., 1991]. The rocks are dominantly amphibolites and gneisses of amphibolite grade metamorphic facies. Detailed descriptions including electrical logs are to be found in Haak et al [1997]. For the purpose of comparison with rocks recovered from the core, an amphibolite (Sp769) from a surface exposure near Spessart, Germany, was also studied. All rocks measured were gneisses or amphibolites having initial porosity less than one volume percent. Measurements were made at a nominal room temperature of $25^\circ C$ on rocks that had been evacuated and then back-saturated with $1\ M\ NaCl$ solution following the method described by Llera et al. [1990]. The $1\ M\ NaCl$ solution was chosen to approximate the electrical conductivity of fluids encountered in the borehole. Conductivity was calculated from resistance measured with an accuracy of 1% as described in detail by Nover et al. [1995]. Figure 1 shows the

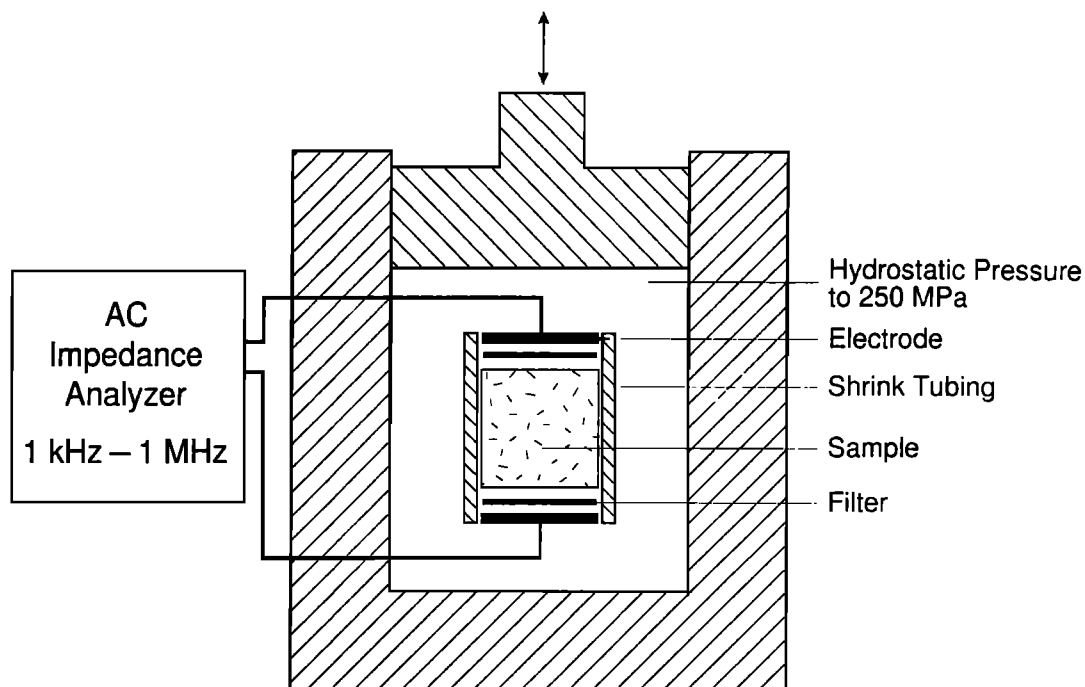


Figure 1. Experimental apparatus for frequency dependent measurements of electrical conductivity in a pressure vessel.

experimental assembly and a schematic of the apparatus used. Because fluid squeezed from the rock by confining pressure could be absorbed into the porous electrodes, the sample was measured in the "drained" condition of constant pore pressure ≈ 1 atm.

The distribution of carbonaceous materials in rocks on the scale of a thin section was determined with the electron microprobe by rastering the electron beam over the analytical surface and simultaneously monitoring carbon X ray intensity. The latter was monitored by crystal spectrometer fitted with a Ovonyx Ni-C (OV95) multilayer diffracting crystal. A 100-Å-thick layer of silver was used as the conductive coat. The procedure is described in detail by *Mathez et al.* [1995]. As emphasized in that work, the electron probe provides a bulk analysis in that the X ray signal emerges from a region a micron or so deep, whereas electron spectroscopies, which have also been brought to bear on the study of carbon in rocks [*Mathez, 1987; Frost et al., 1989; Tingle et al., 1991; Mareschal et al., 1992*], are sensitive to only the upper tens of atomic monolayers of the surface. Because analytical sensitivity of the electron probe for carbon is at best hundreds of ppm, several surface monolayers of carbon compounds are not detectable by this technique. To form visible images in the electron probes, carbon films must be at least tens of nm thick and therefore may represent features of significantly high conductivity.

Thin slabs of rock were flattened on SiC paper and ultrasonically cleaned, the analytical face was polished with alumina/water slurries, and the slabs were mounted on glass slides with conductive carbon tape. The rock slabs were several millimeters thick, eliminating any possibility of contamination by the adhesive. Particulate contamination from the preparation materials or other sources was seldom observed but could easily be identified as isolated spots and imaged by secondary or backscattered electrons. The electron and X ray optics of the electron probe dictated that only small areas could be examined in a single-raster image. Consequently, numerous images of regions ~ 200 μm across were collected for this study. The distribution of accessory minerals, in particular Fe-Ti oxides and sulfides, was examined in detail in all the samples at the thin section to micron scales by backscattered electron (BSE) imaging with a scanning electron microscope.

Results

Petrography

The BSE image of Figure 2 shows features relevant to understanding electrical properties of this suite of samples. First, the quartz (black) and garnet (light gray) are insulators at both the temperature of these experiments and at in situ conditions at the KTB. Second, the ilmenite (along with trace amounts of sphenes and sulfides, all of which appear white) is relatively abundant in the photomicrograph, which is of an oxide-rich layer in a sample having a well-developed fabric. However, the ilmenite does not make an interconnected network more than several hundred microns in length on the two-dimensional analytical surface, and neither the texture nor ilmenite abundance suggest that a significantly larger interconnected network exists in three dimensions. The other two samples examined contain much less ilmenite, sphene or other conductive phases.

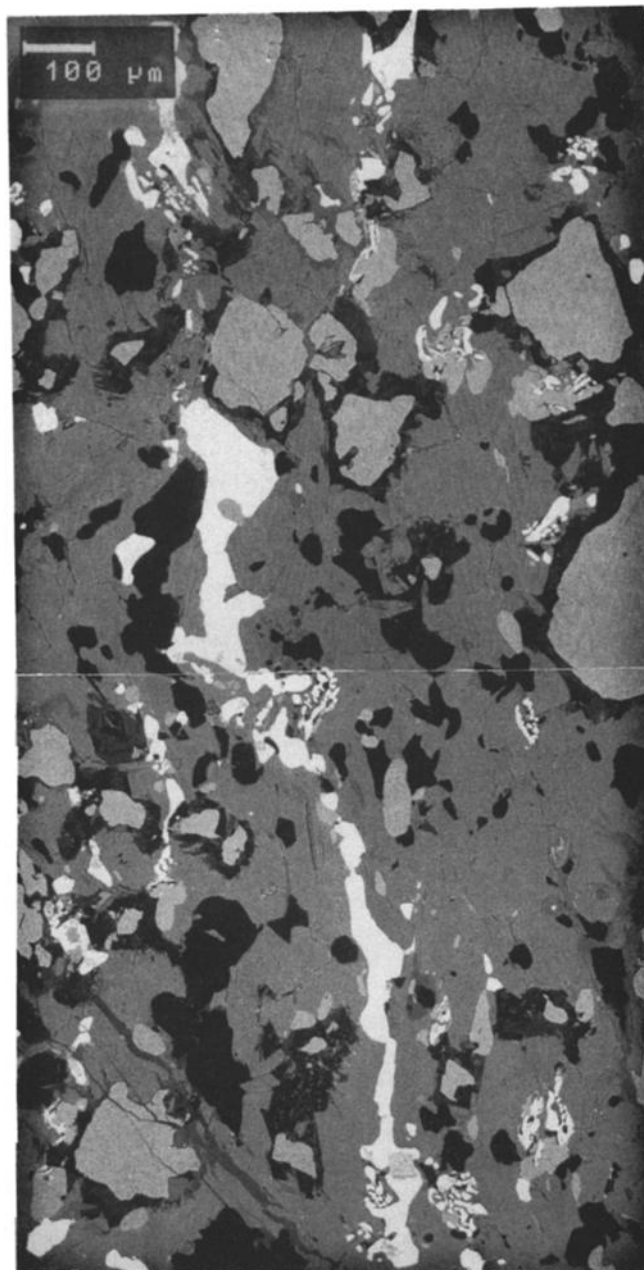


Figure 2. Backscattered electron (BSE) image of amphibolite from sample H006 G52. The black material is quartz; the dark gray mineral is amphibole (with carbon on some of cleavage surfaces); the light gray, granular mineral is almandine-rich garnet, and the white is ilmenite (plus minor sphene and other oxides).

The outstanding feature of the two amphibolites, in which amphibole makes up 40-60% of the mode, is the presence of carbon along planar microfractures (Figure 3). These microfractures are interpreted to be cleavage planes because they intersect at the characteristic amphibole intersection angle of $\sim 120^\circ$. For garnet amphibolite H006 G52, one hundred twelve of the three hundred twenty-six images collected (a third) displayed linear features decorated with carbon. This observation together with the facts that amphibole is the dominant rock-forming mineral and that the carbon forms linear arrays on the

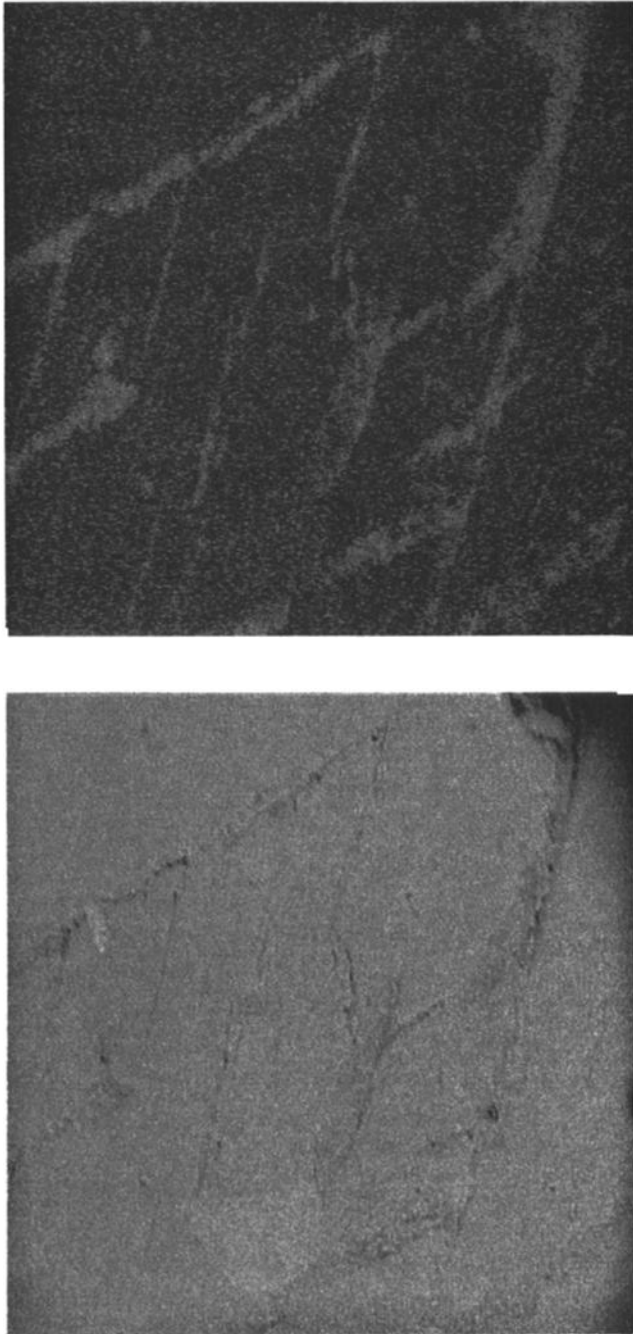


Figure 3. (top) Carbon X ray map on amphibole in sample H006 G52 and (bottom) corresponding BSE image. The cleavage surfaces intersect the analytical surface, exposing the carbon film on the former. The images are 200 μm across.

amphibole analytical surface suggest that the carbon forms a high degree of interconnection and that the two phases together (carbon and ilmenite) must form a network of even greater connectivity.

The precise nature of the carbon phase is not known. Initial attempts to characterize it by static secondary ion mass spectroscopy suggest that the films are composed of complex mixtures of carbons and hydrocarbons. From our electron probe study they are also known to be locally chlorinated, a characteristic of carbons observed on microcracks in other rocks [e.g., Mathez *et al.*, 1995].

Carbon films should not in general have the same electrical conductivity as highly graphitized bulk carbon. Crystallinity and structure as well as conductivity depend greatly on temperature–time history and are usually less than that of highly crystalline graphite [e.g., Spain, 1981]. Evaporated carbon films (which are the most studied but least resemble natural carbons) can have a substantial temperature dependence [Kupperman *et al.*, 1973] but with enough time and temperature develop a “turbostratic” structure of oriented graphitic microcrystals [Oberlin *et al.*, 1975]. Time and temperature act to increase conductivity of such amorphous films [McLintock and Orr, 1973]. In natural materials similar graphitic structures [Pasteris, 1988] or actual graphite have been found [Frost, *et al.*, 1989]. It is not possible to be quantitative about conductivities of carbon in these rocks, but we expect them to be less than that of crystalline graphite ($>10^4 \text{ S m}^{-1}$).

Conductivity

Figures 4 and 5 show representative behaviors of samples subjected to pressure. In Figure 5 are defined the parameters used in this analysis: room pressure conductivity $\sigma(0.1)$, the extrapolated intercept σ_0 of the straight-line fit to the slope at higher pressures, and the logarithmic slope, $d\log_{10}\sigma/dP$. As indicated, the slope comes from the continuous data that occur at somewhat higher pressure after an initial offset. The offset is then the difference $\Delta\sigma_1 = \sigma(0.1) - \sigma_0$ between initial and extrapolated conductivity and can be of either sign.

The textures of Figures 2 and 3 afford a means of visualizing the different observed pressure effects through a simplified conductivity model such as that in Figure 6. The model would apply to samples as recovered and measured in the laboratory and may not necessarily represent the rock in its in situ condition because of differences in salinity of fluid saturant, temperature, and any alteration of crack porosity by coring and extraction. The interconnected portion of any fluid phase would conduct in parallel (and perhaps in series also) with the conducting solid phases shown as carbon-bearing amphibole and ilmenite; the latter is not an interconnected

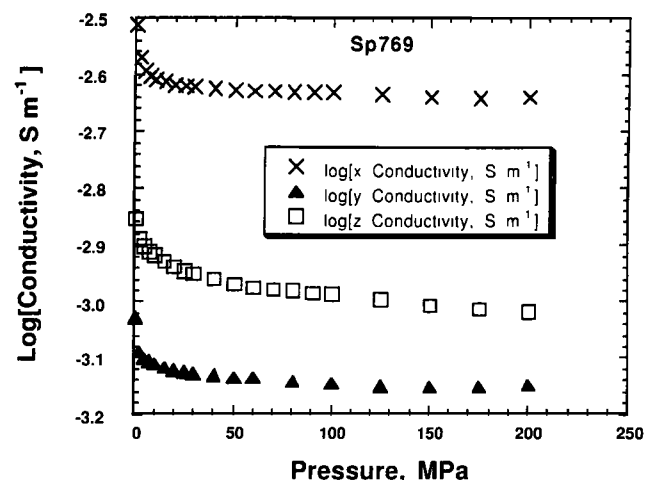


Figure 4. Decreasing conductivity with confining pressure in amphibolite Sp769. The sample, which is similar to those recovered from the German Continental Scientific drilling site (KTB) core, was collected from an outcrop and thus exposed to weathering.

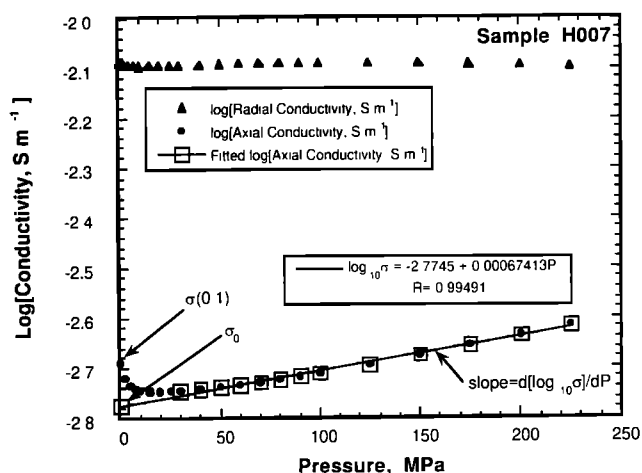


Figure 5. Anisotropic, increasing conductivity with confining pressure in amphibolite sample H007 from 4595 m in the Hauptbohrung. Room pressure conductivity is $\sigma(0.1)$, and σ_0 is the extrapolated intercept of the straight-line fit having slope $d\log_{10}\sigma/dP$. There is an initial offset approximated by the quantity $\Delta\sigma_1 = \sigma(0.1) - \sigma_0$.

phase by itself, but it enhances σ by being in series with conduction through amphibole.

As clearly demonstrated in previous work [e.g., *Brace et al.*, 1965; *Brace and Orange*, 1968; *Hyndman and Drury*, 1976; *Rai and Manghnani*, 1981; *Lockner and Byerlee*, 1985], when conduction is by electrolytic fluids in rock fractures, the effect of confining pressure is to reduce fluid content and thereby to diminish conductivity. Thus the positive or negative sign of the slope of conductivity versus pressure is a diagnostic of conduction mechanism. In Figure 6 the through-going, fluid-filled crack is regarded as more important to conduction than any solid phase and is diminished by confining pressure. Such behavior was measured in the present study on a rock sample (Sp769, Figure 4) similar to the KTB samples but obtained from a surface outcrop. During exhumation and weathering, this sample presumably lost most or all of the delicate surface films that might have been present at depth [*Duba*, 1992; *Katsube and Mareschal*, 1993].

In contrast, the KTB core samples shown here mainly exhibit increased conductivity with pressure. Like Sp769 these specimens are highly anisotropic, but this applies to both sign and magnitude of their pressure shifts. Such behavior is demonstrated in Figure 5. We note that this positive shift is a remarkable result that is not expected to be a simple consequence of the presence of conducting fluids. Indeed, although *Glover and Vine* [1992] observed positive pressure shifts in some dry samples, the shift changed sign to become negative in the presence of fluids. In the picture of Figure 6 the through-going, fluid-filled crack contributes a smaller conductance so that reconnection of solid phase conductors in the crystalline phases (principally amphibole) can overwhelm loss of the fluid conductance. In the other circumstances, which do not apply to these experiments, *Lockner and Byerlee* [1986] observed conductivity increases with time at constant deviatoric stress, but those measurements were made in the dilatant regime of increasing porosity as opposed to the condition of increasing confining pressure and decreasing porosity.

Discussion

In this section we explore further some relationships between measured physical properties and interpret them in terms of rock fabric and conductivity mechanisms. Results from a large number of experiments [see *Nover et al.*, 1995] are summarized in Table 2. The conductivity behavior of rocks demonstrates that simple explanations in terms of a single conducting phase are not sufficient. For instance, frequency dependence of resistivity was interpreted by *Nover et al.* [1995] to yield a constant electronic contribution (from sulfides, oxides, or carbon) in parallel with the electrolytic component.

Pressure-Induced Increase of Conductivity and Reconnection of Solid Conductors

Figure 7 shows a particular feature of samples having positive slopes of $\log\sigma$ versus P : the steeper slopes belong to specimens for which conductivities are low. One simple explanation (Figure 6) is that solid phase conduction takes place in parallel with another mechanism assumed to have negligible or negative pressure effect, most likely a fluid phase in these saturated samples, and that conductivity increases most strongly due to solid phase reconnection when there is less of a fluid phase contribution to offset it. Figure 8 displays this trade-off more clearly: the less the initial conductivity σ_0 , the greater the slope of the positive pressure effect. On the other hand, there is no such trend for samples having negative slopes; for such samples the two parameters are basically uncorrelated. It is consistent with these results to associate the positive pressure effect with solid-phase reconnection and the intercept with conductivity due primarily to a fluid network.

We have insufficient information on sample porosity, other than that it is less than 1%, to relate it to conductivity. However, permeability k , which is also a transport property directly comparable with conductivity because it also requires interconnected porosity, is probably a better measure of through-going fluid pathways. Figure 9, which remarkably resembles Figure 8, illustrates this connection and therefore the association of σ_0 with fluid. It is not surprising, then, that k and σ_0 are found to increase together, as seen in Figure 10. Figure 10 also shows a similar correlation with $\sigma(0.1)$, the other presumed measure of fluid interconnection at low

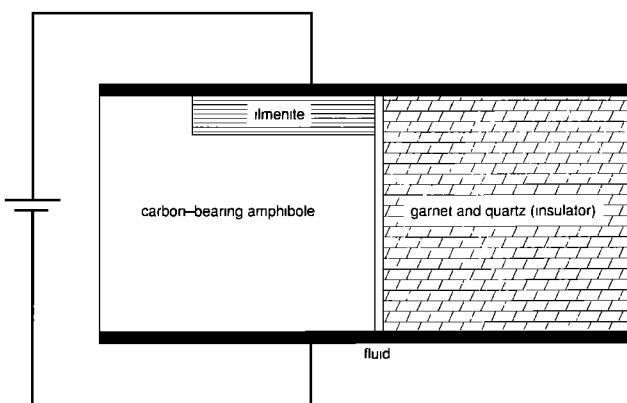


Figure 6. Conductivity model for this amphibolite suite. Carbon-bearing amphibole plus ilmenite conduct in parallel with fluids in cracks and pores.

Table 2. Properties of Samples

Sample	Depth, m	Initial Value $\sigma(0.1 \text{ MPa})$, S m^{-1}	Intercept σ_0 , S m^{-1}	Slope $d\log_{10}\sigma/dP$, MPa^{-1}	Permeability m^2	Ilmenite Plus Sulfides Volume Fraction
H001B20a-A	4150.41	0.001972	0.0011471	-5.9021e-05	1.0E-20*	0.010
H001B20a-R	4150.41	0.0015848	0.0012817	0.00077835	3.0E-20	0.010
H001E44-A	4152.75	0.002243	0.0019829	0.00080060	6.4E-21	0.005
H001E44-R	4152.75	0.0044875	0.0043772	0.00032705	4.52E-17	0.005
H003A4-A	4251.22	0.0068301	0.0062101	0.00081511	3.17E-19	0.017
H003A4-R	4251.22	0.0049855	0.0040225	-0.00070481	2.11E-18	0.038
H004A5-A	4341.99	0.001711	0.0010605	-0.00064419	2.76E-20	0.005
H004A5-R	4341.99	0.0023521	0.0016804	0.0011551	3.75E-20	0.005
H005B20-A	4448.37	0.013083	0.013023	0.00019610	9.0E-19	0.015
H005B20-R	4448.37	0.031656	0.031362	-0.00011127	6.68E-17	0.020
H006G52b-A	4516.60	0.0009798	0.0011489	0.0010152	2.47E-20	0.039
H006G52b-R	4516.60	0.0063194	0.0072761	0.00041664	2.95E-19	0.078
H007C25-A	4594.64	0.0020354	0.0016807	0.00067406	2.4E-20	
H007C25-R	4594.64	0.0081984	0.0081003	-5.6796e-07	7.10E-17	
H008B22-A	4647.47	0.014774	0.015424	-7.0175e-05	1.55E-18	
H008B22-R	4647.47	0.017821	0.018327	0.00014512	2.04E-18	
H009B11-A	4685.55	0.001699	0.0014401	0.00075653	5.0E-21	
H009B11-R	4685.55	0.010529	0.010693	-0.00022751	5.57E-17	
H010C28-A	4822.23	0.0024846	0.0022351	0.00034268	3.44E-17	
H010C28-R	4822.23	0.00663	0.0049762	-0.00062630	5.23E-19	
H011A8-A	5012.52	0.0016083	0.0012981	0.00069352		
H011A8-R	5012.52	0.0015917	0.0012936	0.00073320	9.61E-17	
H031-AltP1	7011.97	0.02921	0.028445	-0.00040904		
H031-AltP2	7011.98	0.0048075	0.0042815	-0.00015264		
H031-B4gP1	7012.19	0.10536	0.063009	-8.0279e-05		
H031-B4yP1	7012.86	0.013275	0.0062431	-0.00015353		
H031-B4yP2	7012.84	0.012216	0.012045	-0.00073274		
H031-B4yP3	7012.90	0.011724	0.0054338	-0.0051074		
H031-B4yP4	7012.81	0.0060237	0.0056520	0.00044009		
H031-B4zP1	7012.80	0.013275	0.0033620	-0.00087542		
VB284x	1360.00	0.0016757	0.0014602	0.00086580	7.90E-19	
VB284y	1360.00	0.0012026	0.00070437	7.5331e-05	7.40E-20	
VB284z	1360.00	0.00064268	0.00040235	0.0011634	2.47E-20	
VB420x	1858.00	0.017983	0.020221	-0.00019777		
VB420y	1858.00	0.0056101	0.0065373	0.00023262		
VB420z	1858.00	0.0012007	0.00032862	0.0018107		
VB767x	3145.00	0.0049832	0.0041505	0.00017662	2.37E-17	
VB767y	3145.00	0.0023436	0.0021822	-0.00022827	1.0E-19	
VB767z	3145.00	0.0011995	0.00078560	0.0010128	1.3E-20	
VB769x	3150.00	0.0030886	0.0023851	-8.2699e-05	2.17E-18	
VB769y	3150.00	0.00093898	0.00073773	0.00010304		
VB769z	3150.00	0.0014042	0.0011115	-0.00032630		

VB samples are from the preliminary drill hole (Vorbohrung), and HBO samples are from the main drillhole (Hauptbohrung). Sample suffix A means a core parallel to core axis; suffix R means a core along a radius.

*Read 1.0E-20 as 1.0×10^{-20}

pressure. In this case, the relationships hold regardless of slope of the pressure effect, another indication that solid phases have only a minor influence on $\sigma(0.1)$ and σ_0 . The slightly better correlation for the case of negative $d\log_{10}\sigma/dP$ is another hint that curves with positive slope indicate the presence of solid conductors. As a final hint, we note that both parts of Figure 10 have a property predicted from models of conductivity and permeability. For simple parallel crack porosity a conceivable approximation for rocks that have been cooled, decompressed, and fractured, fluid-phase conductivity increases as microcrack aperture w , and k increases as w^3 on the assumption that the samples differ principally in their apertures [e.g., Fox and McDonald, 1985; Guégen and Palciauskas, 1994]. Hence a plot of σ_0 versus k should show $\sigma_0 \propto k^{1/3}$, a relationship approximated by the data in Figure 10. Curves showing similar power law relations between

conductivity and permeability when conduction takes place in the fluid phase have frequently been demonstrated [e.g., Brace et al., 1968; Brace, 1977; Lockner and Byerlee, 1985; Morrow et al., 1994]. Different power law slopes apply depending on assumptions of pore shape and configuration [David, 1993], with typical values in the range 1/3 to 1 [Walsh and Brace, 1984].

We would expect that fluid-phase conduction in rocks in situ should be less than in laboratory samples because compression in the laboratory does not exactly reverse the previous expansion due to decompression and anisotropic contraction due to cooling during core extraction. Therefore the rocks should have had lower porosity at depth than in the laboratory and less of a fluid component of conductivity. Correspondingly, the necessarily imperfect reconnection of solid phases in the laboratory would mean that this

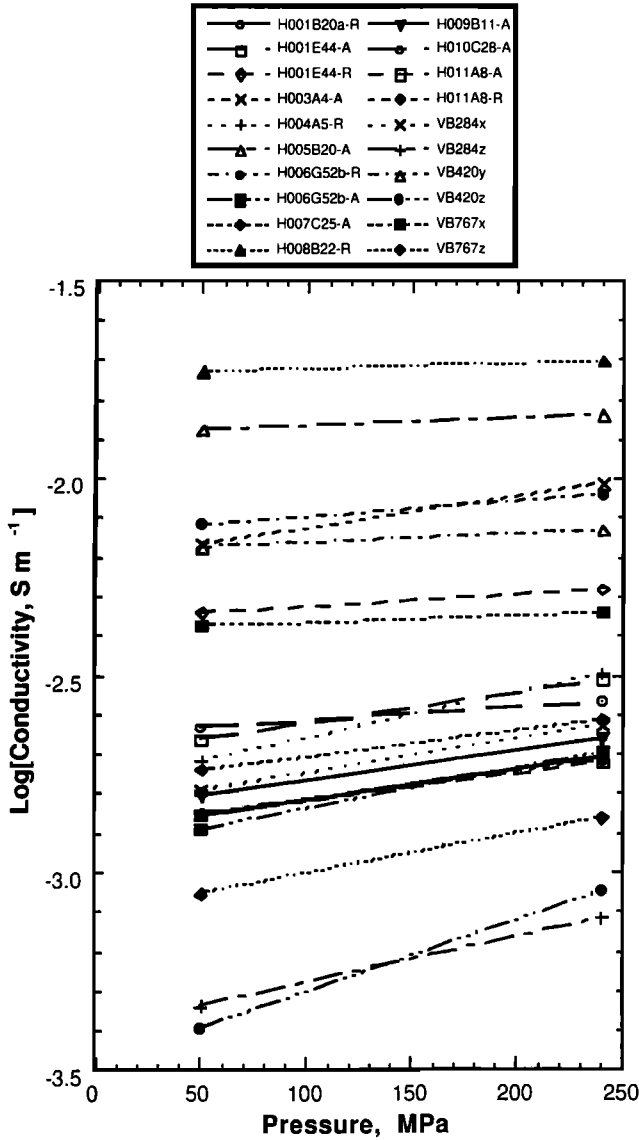


Figure 7. Logarithms of conductivities at pressures of 50 and 240 MPa for samples having positive slopes. Curves of low conductivity display steeper slopes.

component should have been stronger before the rocks were removed to the surface.

Percolation Interpretation

The hypothesis that positive pressure shifts result from reconnection of solid conductors in the rock is unusually well suited for interpretation by percolation theory. A classic example [Shankland and Waff, 1974; Zallen, 1983] is the resistor network of Figure 11a. When a fraction p of bonds (links) is cut from the mesh, conductance of the mesh is reduced in a linear way until a critical fraction p_c is reached, no connected path remains, and conductance drops to zero.

In the model proposed here the interconnected pathways of carbonaceous conducting films on grain boundaries or cleavage surfaces, such as those shown in Figure 3, were partially broken in the course of core extraction so that conductivity is at an intermediate condition less than the undisturbed state, hence somewhere along the slope of Figure

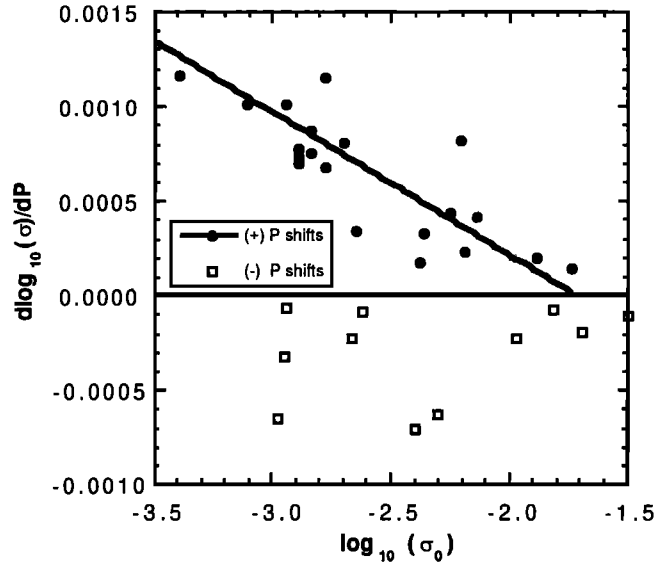


Figure 8. Slopes of pressure effect versus intercept σ_0 . In contrast with uncorrelated behavior for samples having negative slopes, samples of positive slopes show a trade-off of $d\log_{10}\sigma/dP$ with σ_0 .

11b. (Except for cases of unusually carbon-rich rocks, we would expect nearly all the solid interconnections to be lost in weathered outcrop rocks such as those normally examined, for example, Sp769 of Figure 5. It is the freshness of the KTB rocks that makes them essential for these studies.)

The model presumes that confining pressure restores a fraction of the interconnections. Bond percolation formulas are of the form

$$\frac{\sigma}{\sigma_m} = \frac{p - p_0}{1 - p_0} \quad (1)$$

where p_0 is a fraction close to p_c and σ_m is conductivity at maximum interconnection [Shankland and Waff, 1974]. To

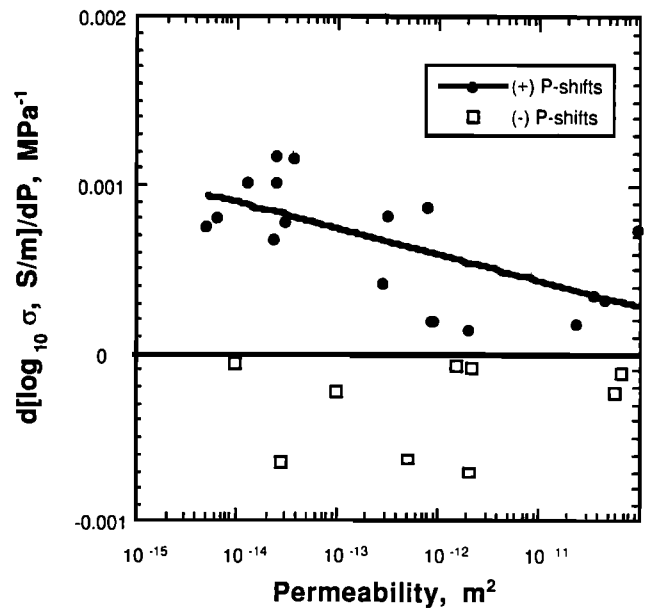


Figure 9. Slopes of pressure effect versus permeability k showing how k has a relationship to slope similar to that of σ_0 in Figure 8.

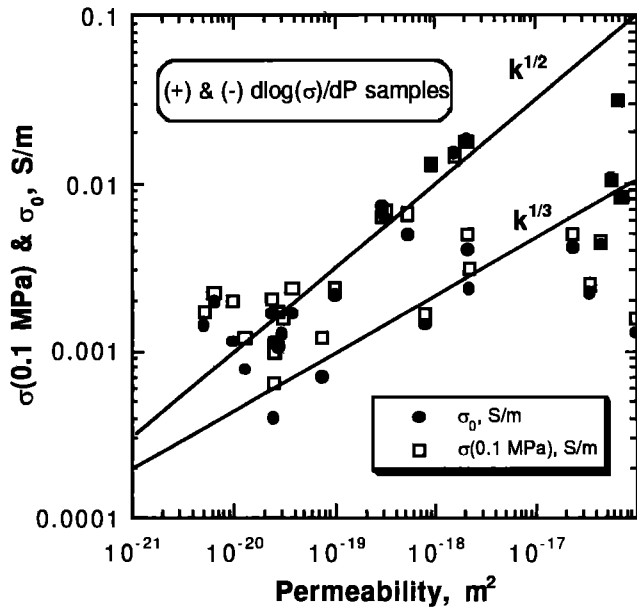


Figure 10. The relationships between room pressure conductivity $\sigma(0.1)$ and intercept σ_0 with permeability k illustrates the relationship between these fluid-dominated properties. Although there is little difference between samples of positive $d\log_{10}\sigma/dP$ and samples of negative $d\log_{10}\sigma/dP$, separate analysis shows the latter to be slightly better correlated. Slopes such that $\sigma_0 \propto k^{1/3}$ and $k^{1/2}$ illustrate suggested dependences upon crack aperture.

estimate the reconnection rate, we can differentiate (1):

$$\frac{1}{\sigma_m} \frac{d\sigma}{dP} = \frac{1}{1 - p_0} \frac{dp}{dP} \quad (2)$$

Approximating a few values such that $p_0 \approx 0.33$ and the slope $d\log_{10}\sigma/dP = 1 \times 10^{-3} \text{ MPa}^{-1}$, which are typical values, yields

$$\frac{1}{\sigma_m} \frac{d\sigma}{dP} \approx \frac{d\ln\sigma}{dP} \approx 2.3 \frac{d\log\sigma}{dP} \approx +2.3 \times 10^{-3} \approx 1.3 \frac{dp}{dP} \quad ,$$

or,

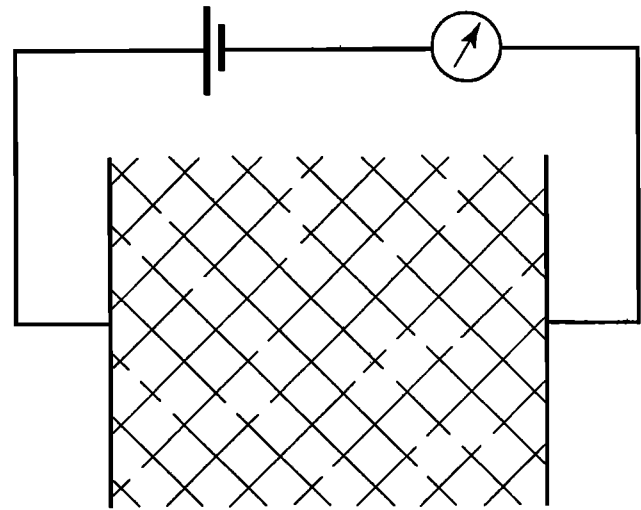
$$\frac{dp}{dP} \approx 2 \times 10^{-3} \text{ MPa}^{-1} \quad (3)$$

as the fraction of broken bonds restored by increasing pressure in the experiments. Of course this is a rough estimation for the parameters of the percolation model and not necessarily the rate that would occur in situ, because it is not possible to precisely reverse changes caused by core extraction. However, the advantage of using KTB samples is that core extraction should be less disturbing of carbon texture in the rock fabric than would be the exposure process at geological rates.

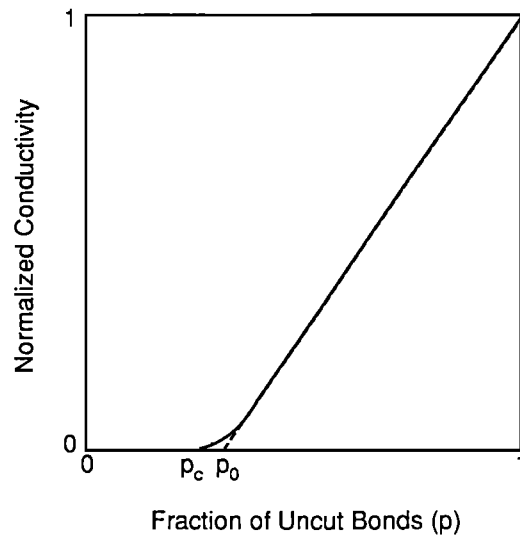
Contributions From Oxides and Sulfides

Highly conducting Fe-Ti oxides, principally ilmenite plus trace quantities of sulfide, are present in most of these rocks in significant volume fractions of 0.01-0.08, but their texture imposes difficult requirements for interconnection. When a mesh of conducting elements is used to model conducting elements, the shape of the elements is important. For example, to achieve a p_c of 0.25, which is the minimum value for interconnection in a roughly cubic, three-dimensional

network, more than 25% of quasi-planar carbon films as conducting elements must make contact, but the volume fraction of carbon can still be low. However, when the conducting elements are roughly spheres or euhedral crystals, then a volume fraction greater than 25% is necessary to form an interconnection. As noted above, the ilmenite in the KTB rocks, although it locally takes part in the definition of the fabric, appears not to form an interconnected network in two or three dimensions. Even allowing for slight anisotropy in the rock fabric to enhance the possibility of interconnection, it is difficult to imagine that a volume fraction of the order of 0.01-0.08 could form an interconnected phase by itself. For this reason, the ilmenite is shown as being in series with the carbon-bearing amphibole in the simple model of Figure 6. The interpretation that carbon must take part in establishing connectivity with increasing pressure is further supported by the fact that we find no correlation of σ_0 or $d\log\sigma/dP$ with abundances of ilmenite and sulfides.



(a)



(b)

Figure 11. (a) Two dimensional model of a percolation mesh and (b) normalized conductivity of the mesh as a function of the fraction of uncut bonds.

Contributions From Fluids

An alternative interpretation is that the increase in conductivity with pressure is due to redistribution of fluid-filled cracks into a phase of better interconnection [Rauen *et al.*, 1994]. The pressure-induced phase would presumably more closely resemble that of films, that is, flatter cracks of lower total porosity. However, application of hydrostatic (as opposed to uniaxial) pressure acts to close cracks, and flatter cracks are the first to close on application of confining pressure [Walsh, 1965; Walsh and Grosebaugh, 1979].

It is possible to consider other fluid-based causes for a positive pressure shift. For instance, in the unlikely event of only partial saturation in some samples and perhaps poor wetting by the fluid, then pressure might force improved interconnection leading to a positive pressure shift. However, in this case we might expect an initial positive offset $\Delta\sigma_1 = \sigma(0.1) - \sigma_0$ (defined in Figure 5), but this should then be followed by a turnover to negative slope as porosity decreases at higher confining pressures. Yet the higher pressure slopes defined in Figure 5 are the ones that are plotted and decrease with fluid contribution at higher permeabilities (Figure 9). Another argument against this hypothesis is that permeability in the KTB samples decreases monotonically with pressure in all cases [Nover *et al.*, 1995]. A simpler explanation for the positive offsets might be that ilmenite is involved and makes its own better contacts through initial bridging with water and carbon such that it affects conductivity most strongly at the lowest pressures. Also, many other rocks [e.g., Brace *et al.*, 1965; Brace and Orange, 1968] were of similar low (less than 1%) porosity and as difficult to saturate, so effects of reconnecting imperfectly saturated porosity are not anticipated. If it were possible to repeat these experiments when the carbon films weathered away after several years, loss of the positive pressure shift would be consistent with the carbon conductor hypothesis.

Finally, the process of core extraction should introduce porosity through decompression and cooling and cause breaking of solid phase interconnections. It is probably not possible to apply confining pressure in the laboratory to reverse this process that also breaks solid interconnections. However, such changes have the effect of enhancing fluid contributions over those of solid conductors in laboratory conditions. Hence the principal conclusion that a positive pressure shift of conductivity is an indicator of the solid reconnection is strengthened by the present observations.

We checked for other relationships. No discernible correlations were found between slopes, intercepts, mineralogy, and quantities such as depth of origin of each core.

Conclusions

Measurements on KTB samples have afforded a rare opportunity to look into the midcrust under conditions much closer to those ordinarily available in the laboratory. They have made possible the observation of a previously rare positive pressure effect on electrical conductivity for which the simplest explanation is interconnected solid phase conducting elements. In the KTB rocks it appears to be the presence of carbon on the planar cleavage surfaces in one of the rock-forming minerals (amphibole) assisted by a good conductor (ilmenite) and some fluids that yield high

conductivity. This work shows that the relatively high midcrustal conductivity seen in the Bohemian Massif can be dominated by solid conductors to yield conductivities of order 10^{-2} S m^{-1} as described by Haak *et al.* [1991]. If we also consider the general question of how much mid to lower crustal conductivity can be attributed to solid phases, we must ask how representative this region is of "typical" crust. Is the solid phase inferred for these rocks likely to be a widespread phenomenon or in comparison with free fluid phases [Hyndman *et al.*, 1993]? Carbon films on microfracture surfaces have been observed in a variety of rocks and may be common. Yet it remains to be demonstrated that carbon or oxides are everywhere present in continental crust.

Acknowledgments. We gratefully thank G. Nover and S. Heiamp of the Mineralogisches Institut, Universität Bonn, Germany, for supplying experimental data for this analysis and the KTB Feldlabor, Windischeschenbach, Germany for providing samples for texture analysis. The manuscript was improved by helpful comments from George Jiracek and Gary Olhoeft. AGD thanks the Département des Géomateriaux of the Institut de Physique du Globe de Paris for generous hospitality during preparation of this manuscript. This work was supported by grants from the Geosciences Research Program, Office of Basic Energy Sciences of the Department of Energy with assistance from the Los Alamos Branch of the Institute of Geophysics and Planetary Physics.

References

- Alabi, A. O., P. A. Camfield, and D. I. Gough, The North American central plains conductivity anomaly, *Geophys. J. R. Astron. Soc.*, **43**, 815-833, 1975.
- Bailey, R.C., J. A. Craven, J. C. Macnae, and B. D. Polzer, Imaging of deep fluids in Archaean crust, *Nature*, **340**, 136-138, 1989.
- Brace, W. F., Resistivity of saturated crustal rocks to 40 km based on laboratory studies in *The Structure and Physical Properties of the Earth's Crust*, *Geophys. Monogr. Ser.*, vol. 14, edited by J. G. Heacock, 169-184, AGU, Washington, D.C., 1971.
- Brace, W. F., Permeability from resistivity and pore shape, *J. Geophys. Res.*, **82**, 3343-3349, 1977.
- Brace, W. F., and A. S. Orange, Further studies of the effects of pressure on electrical resistivity of rocks, *J. Geophys. Res.*, **73**, 5407-5420, 1968.
- Brace, W. F., A. S. Orange, and T. R. Madden, The effect of pressure on the electrical resistivity of water-saturated crystalline rocks, *J. Geophys. Res.*, **70**, 5669-5678, 1965.
- Brace, W. F., J. B. Walsh, and W. T. Frangos, Permeability of granite under high pressure, *J. Geophys. Res.*, **73**, 2225-2236, 1968.
- David, C., Geometry of flow paths for fluid transport in rocks, *J. Geophys. Res.*, **98**, 12,267-12,278, 1993.
- Duba, A. G., Grain-boundary carbon can cause conductivity anomalies (abstract), *Eos Trans. AGU*, **73** (43), Fall Meet. Suppl., 240, 1992.
- Duba, A., E. Huenges, G. Nover, G. Will, and H. Jödicke, Impedance of black shale from Münsterland 1 borehole: An anomalously good conductor?, *Geophys. J.*, **94**, 413-419, 1988.
- Duba, A., S. Heikamp, W. Meurer, G. Nover, and G. Will, Evidence from borehole samples for the role of accessory minerals in lower-crustal conductivity, *Nature*, **367**, 59-61, 1994.
- ELEKTB Group, KTB and the electrical conductivity of the crust, *J. Geophys. Res.*, **102**, in press, 1997.
- Emmermann, R., A. Duba, and J. Lauterjung, Continental scientific drilling in Germany: Attempts to attain at least 10,000 m, *Eos Trans. AGU*, **72**, 193-197, 1991.
- Fox, R. W., and A. T. McDonald, *Introduction to Fluid Mechanics*, 3rd ed., chap. 8, John Wiley, New York, 1985.
- Frost, B. R., and K. Bucher, Is water responsible for geophysical anomalies in the deep continental crust? A petrological perspective, *Tectonophysics*, **231**, 293-309, 1994.
- Frost, B. R., W.S. Fyfe, K. Tazaki, and T. Chan, Grain-boundary graphite in rocks and implications for high electrical conductivity in the lower crust, *Nature*, **340**, 134-136, 1989.
- Glover, P. W. J., and F. J. Vine, Electrical conductivity of carbon-

- bearing granulite at raised temperatures and pressures, *Nature*, 360, 723-726, 1992.
- Gough, D. I., Seismic reflectors, conductivity, water, and stress in the continental crust, *Nature*, 323, 143-144, 1986.
- Guégen, Y., and V. Palciauskas, *Introduction to the Physics of Rocks*, chap. 5 and 8, Princeton Univ. Press, Princeton, N.J., 1994.
- Haak, V., and R. Hutton, Electrical resistivity in continental lower crust, in *The Nature of the Lower Continental Crust*, edited by J.B. Dawson, D.A. Carswell, J. Hall, and K.S. Wedepohl, Geol. Soc. Spec. Publ., 24, pp. 35-49, 1986.
- Haak, V., J. Stoll, and H. Winter, Why is the electrical resistivity around the KTB hole so low?, *Phys. Earth Planet. Inter.*, 66, 12-23, 1991.
- Hyndman, R. D., and M. J. Drury, The physical properties of oceanic basement rocks from deep drilling on the Mid-Atlantic Ridge, *J. Geophys. Res.*, 81, 4042-4052, 1976.
- Hyndman, R. D., and P. M. Shearer, Water in the lower continental crust: Modelling magnetotelluric and seismic reflection results, *Geophys. J. Int.*, 98, 343-365, 1989.
- Hyndman, R. D., L. L. Vanyan, G. Marquis, and L. K. Law, The origin of electrically conductive lower continental crust: Saline water or graphite?, *Phys. Earth Planet. Inter.*, 81, 325-344, 1993.
- Jiracek, G. R., Geoelectromagnetics charges on, *Revs. Geophys.*, 33, Suppl., 169-176, 1995.
- Jiracek, G. R., V. Haak, and K. H. Olsen, Practical magnetotellurics in a continental rift environment, in *Continental Rifts: Evolution, Structure and Tectonics*, pp. 103-129, edited by K. H., Olsen, Elsevier, New York, 1995.
- Jödicke, H., Water and graphite in the earth's crust--An approach to interpretation of conductivity models, *Surv. Geophys.*, 13, 381-407, 1992.
- Jones, A. G., Electrical properties of the continental lower crust, in *The Lower Continental Crust*, edited by D. M. Fountain, R. J. Arculus and R. W. Kay, pp. 81-143, Elsevier, New York, 1992.
- Kariya, K. A., and T. J. Shankland, Electrical conductivity of dry lower crustal rocks, *Geophysics*, 48, 52-61, 1983.
- Katsube, T. J., and M. Mareschal, Petrophysical model of deep electrical conductors: Graphite lining as a source and its disconnection due to uplift, *J. Geophys. Res.*, 98, 8019-8030, 1993.
- Kupperman, D. S., C. K. Chau, and H. Weinstock, Electrical resistivity of carbon films, *Carbon*, 11, 171-175, 1973.
- Lee, C. D., F. J. Vine, and R. G. Ross, Electrical conductivity models for the continental crust based on laboratory measurements on high-grade metamorphic rocks, *Geophys. J. R. Astron. Soc.* 72, 353-371, 1983.
- Llera, F.J., M. Sato, K. Nakatsuka, and H. Yokoyama, Temperature dependence of the electrical resistivity of water-saturated rocks, 55, 576-585, 1990.
- Lockner, D. A., and J. D. Byerlee, Complex resistivity measurements of confined rock, *J. Geophys. Res.*, 90, 7837-7847, 1985.
- Lockner, D. A., and J. D. Byerlee, Changes in complex resistivity during creep in granite, *Pure Appl. Geophys.* 124, 659-676, 1986.
- Losecke, W., K. Knödel, and W. Müller, The conductivity distribution in North German sedimentary basin derived from widely spaced aerial magnetotelluric measurements, *Geophys. J. R. Astron. Soc.* 58, 169-179, 1979.
- Madden, T. R., Random networks and mixing laws, *Geophysics*, 41, 1104-1125, 1976.
- Mareschal, M., W. S. Fyfe, J. Percival, and T. Chan, Grain-boundary graphite in Kapuskasing gneisses and implications for lower-crustal conductivity, *Nature*, 357, 674-676, 1992.
- Mathez, E. A., Carbonaceous matter in mantle xenoliths: Composition and relevance to the isotopes, *Geochim. Cosmochim. Acta*, 51, 2339-2347, 1987.
- Mathez, E. A., and J. R. Delaney, The nature and distribution of carbon in submarine basalts and peridotite nodules, *Earth Planet. Sci. Lett.*, 56, 217-232, 1981.
- Mathez, E.A., A. G. Duba, C. L. Peach, A. Léger, T. J. Shankland, and G. Plafker, Electrical conductivity and carbon in metamorphic rocks of the Yukon-Tanana terrane, Alaska, *J. Geophys. Res.*, 100, 10,187-10,196, 1995.
- McLintock, I. S., and J. C. Orr, Evaporated carbon films, in *Chemistry and Physics of Carbon*, vol. 11, edited by P. L. Walker Jr., and P. A. Thrower, pp. 243-312, Marcel Dekker, New York, 1973.
- Morrow, C., D. Lockner, S. Hickman, M. Susanov, and T. Röckel, *J. Geophys. Res.*, 99, 7263-7274, 1994.
- Nover, G., S. Heikamp, A. Kontny, and A. Duba, The effect of pressure on the electrical conductivity of KTB rocks, *Surv. Geophys.*, 16, 63-81, 1995.
- Oberlin, A., M. Oberlin, and M. Maubois, Study of thin amorphous and crystalline carbon films by electron microscopy, *Philos. Mag.*, 32, 833-846, 1975.
- Olhoeft, G. R., Electrical properties of granite with implications for the lower crust, *J. Geophys. Res.*, 86, 931-936, 1981a.
- Olhoeft, G. R., Electrical properties of rocks, in *Physical Properties of Rocks and Minerals*, edited by N. S. Touloukian, W. R. Judd, and R. R. Roy, pp 257-328, McGraw-Hill, New York, 1981b.
- Pasteris, J. D., Secondary graphitization in mantle-derived rocks, *Geology*, 16, 804-807, 1988.
- Rai, C., and M. Manghnani, The effects of saturant salinity and pressure on the electrical resistivity of Hawaiian basalts, *Geophys. J. R. Astron. Soc.*, 65, 395-405, 1981.
- Rauen, A., J. Duyster, S. Heikamp, A. Kontny, G. Nover, and T. Roeckel, Electrical conductivity of a KTB core from 7000 m—Effects of cracks and ore minerals, *Sci. Drill.*, 4, 197-206, 1994.
- Sanders, I. S., Exhumed lower crust in NW Ireland, and a model for crustal conductivity, *J. Geol. Soc. London*, 148, 131-135, 1991.
- Schwarz, G., Electrical conductivity of the Earth's crust and upper mantle, *Surv. Geophys.*, 11, 133-161, 1990.
- Shankland, T. J., and M. E. Ander, Electrical conductivity, temperatures, and fluids in the lower crust, *J. Geophys. Res.*, 88, 9475-9484, 1983.
- Shankland, T. J., and H. S. Waff, Conductivity in fluid bearing rocks, *J. Geophys. Res.*, 79, 4863-4868, 1974.
- Spain, I. L., The electronic transport properties of graphite, carbons, and related materials, in *Chemistry and Physics of Carbon*, vol. 16, edited by P. L. Walker Jr., and P. A. Thrower, pp. 119-304, Marcel Dekker, New York, 1981.
- Sternberg, B. K., Electrical resistivity structure of the crust in the southern extension of the Canadian Shield—Layered Earth models, *J. Geophys. Res.*, 84, 212-228, 1979.
- Tingle, T. N., E. A. Mathez, and M. Hochella, Carbonaceous matter in peridotites and basalts studied by XPS, SALI and LEED, *Geochim. Cosmochim. Acta*, 55, 1345-1352, 1991.
- Waff, H. S., Theoretical considerations of electrical conductivity in a partially molten mantle and implications for geothermometry, *J. Geophys. Res.*, 79, 4003-4010, 1974.
- Walsh, J. B., The effect of cracks on the compressibility of rocks, *J. Geophys. Res.*, 70, 381-389, 1965.
- Walsh, J. B., and W. F. Brace, The effect of pressure on porosity and the transport properties of rocks, *J. Geophys. Res.*, 89, 931-936, 1984.
- Walsh, J. B., and M. A. Grosenbaugh, A new model for analyzing the effect of fractures on compressibility, *J. Geophys. Res.*, 84, 3532-3536, 1979.
- Walther, J., and E. Althaus, Graphite deposition in tectonically mobilized fault planes of the KTB Pilot Drill Hole, *KTB Rep.* 93-2, pp. 455-460, Schweitzerbart'sche Verlagsbuchhandlung, Stuttgart, 1993.
- Zallen, R., *The Physics of Amorphous Solids*, chap. 4, John Wiley, New York, 1983.

A. G. Duba, Geosciences and Global Security Program, Lawrence Livermore National Laboratory, Livermore, CA 94550; tel 510-422-7306, fax 510-423-1057. (e-mail: alduba@llnl.gov)

E. A. Mathez, Department of Earth and Planetary Sciences, American Museum of Natural History, New York, NY 10024-5192; tel 212-769-5379. (e-mail: mathez@amnh.org)

C. L. Peach, Sea Education Association, P.O. Box 6, Woods Hole, MA 02543. (e-mail: cpeach@sea.edu)

T. J. Shankland, Earth and Environmental Science Division, Los Alamos National Laboratory, Los Alamos, NM 87545; tel 505-667-4907, fax 505-667-8487. (e-mail: shankland@lanl.gov)

(Received March 5, 1996; revised October 11, 1996; accepted October 31, 1996.)